Deformation of a Chromatographic Bed during Steady-State Liquid Flow

Karin C. E. Östergren, A. Christian Trägårdh, Gisle G. Enstad, and Jostein Mosby
Dept. of Food Engineering, Lund University, S-221 00 Sweden

A two-dimensional model was developed that describes the deformation of an open, mechanically stable chromatographic bed during steady-state flow. It is based on the assumption of pure elastic deformation and the validity of Darcy's law. A control-volume method was used to solve the mathematical equations. The computed pressure profiles agree well with experimental data. Computer simulations indicate that radial void variations, which will cause significant flow variations, may occur under chromatographic flow conditions. A method of measuring Young's modulus and the Poisson ratio in a water-saturated sample at very low stress levels (< 15 kPa) using a cubic plane strain tester, is also presented.

Introduction

The successful design and operation of a chromatographic process requires a proper understanding of the kinetics and mass transport, as well as the hydrodynamics in the system under investigation. Although there are a great many rigid chromatographic supports on the market, soft gels, commonly based on cross-linked agarose or dextran, are uniquely useful for the separation of large water-soluble molecules, such as proteins (e.g., Boschetti, 1994).

It is important to be able to predict the pressure drop in a chromatographic column containing nonrigid particles, since the pressure loss during flow is taken up by the solid phase, causing compression of the chromatographic bed, which will limit the range of possible flow rates. Predicting the pressure drop and the degree of compression is a complex task, since the hydrodynamics is intimately coupled with the mechanics of the solid phase.

The friction between the wall and the solid grains will cause a reduction in solid stress such that the stress at a certain depth in the column will always be less than that predicted in an infinitely wide column. The increase in column diameter will decrease the influence of the wall friction. According to Sofer and Nyström (1989) the linear flow rate may decrease to nearly half of its original value when increasing the column diameter from 0.026 m to 0.10 m. Tiller and Lu (1972) showed that the side-wall friction may cause significant radial stress variations in compression–permeability cells having diameters typical for preparative chromatographic columns.

The prediction of the hydrodynamic dispersion is important, since it may influence the resolution of the chromatographic zones. The hydrodynamic dispersion is influenced by the packing structure. According to Charlaix et al. (1987), the local hydrodynamic dispersion in sintered samples that have void fractions between 0.14 and 0.34 was up to 60 times higher than that in an unconsolidated sample. Radial stress variations in a compressed chromatographic column may also cause velocity variations, which will increase the overall hydrodynamic dispersion and thus reduce the efficiency of the chromatographic process. Velocity variations with a maximum to minimum ratio as small as 1.10 were found to cause considerable changes in band profiles in liquid chromatography, according to simulations performed by Yun and Guiochon (1994). To fully understand the sources of the increased overall hydrodynamic dispersion in a compressible chromatographic column, knowledge of the velocity field is essential. The models used so far to predict flow and pressure drop in nonrigid chromatographic systems have been one-dimensional, and cannot be used to investigate the effects of the compression on the velocity field and chromatographic band broadening.

The purpose of this work was to develop a basis for a two-dimensional model that could predict the velocity field in a compressed chromatographic bed. Methods of characterizing

Correspondence concerning this article should be addressed to K. C. E. Östergren.
Current address for G. G. Enstad and J. Mosby: Telemark Technological Research and Development Center, Dept. of Powder Science and Technology (POSTEC), Kjølnes Ring, N-3914 Porsgrunn, Norway.

the solid phase were developed. The compaction of a chromatographic medium during flow was experimentally investigated in an open chromatographic column. The flow and compaction were simulated using a two-dimensional mathematical model. Predicted and experimental data were compared.

Liquid flow through a compressible chromatographic bed

Liquid flow through nonrigid particulate beds has been investigated in different engineering disciplines such as soil science, geotechnology, and chemical engineering. In the field of chemical engineering, work has been performed aimed at modeling and understanding filtration processes (e.g., Shirato et al., 1968; Tiller and Lu, 1972); the wet pressing process of, for example, paper (e.g., Jönsson and Jönsson, 1992); and to predict the pressure drop in a chromatographic column (Jostrua et al., 1967; Verhoff and Furjanic, 1983; Davies and Bellhouse, 1989; Mohammad et al., 1992).

In liquid chromatography the flow rate is generally low, and the pressure drop is proportional to the flow rate and inversely proportional to the viscosity, according to Darcy's law (Bird et al., 1960):

$$U_0 = -\frac{1}{\mu} k \nabla P, \tag{1}$$

where

$$\nabla P = \nabla p - \rho g, \tag{2}$$

U_o is the superficial velocity; μ the viscosity; p the fluid pressure; ρ the fluid density; and k is the permeability, which is related to the structure of the interstitial space of the chromatographic bed. The permeability is usually described as a function of particle diameter and interstitial volume fraction (void fraction) of the packed bed. In the general case, the permeability is a tensor, but under isotropic conditions, the permeability tensor reduces to a scalar. For a rigid chromatographic column the pressure drop will vary linearly along the column, and for a given degree of packing the pressure drop can easily be calculated for any column dimensions. Under compression the situation is different: the void fraction and the overall structure of the gel will depend on the flow rate. The solid stress and thus the structure of the gel will change in the axial direction, due to the fluid stress, as well as in the radial direction, due to the wall friction. The shear stress caused by the friction at the wall is described by (Jenike, 1964):

$$\sigma_w = C_w + \sigma_r \mu_f, \tag{3}$$

where μ_f is the wall friction coefficient, σ_r is the solid stress acting in the radial direction, and C_w describes the adhesion at the wall. The wall friction always opposes the motion at compaction and expansion. The transmission of the stress to the interior of the column is governed by mechanical properties of the gel. Thus, in the general case, the variations in the local structure and the local permeability in both the radial and axial directions must be taken into account in order to calculate the pressure drop in a compressible chromatographic column.

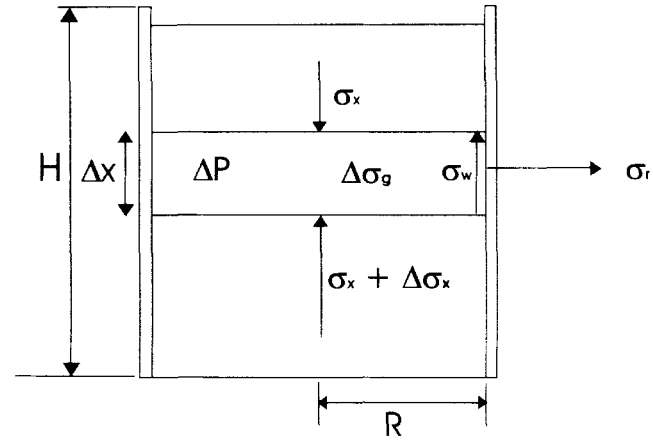

Figure 1. Forces acting on an axial segment of a compressible particulate column during flow, according to the Janssen model.

ΔP is the pressure loss in the fluid phase; $\Delta \sigma_g$ is the gravitational force; σ_w is the frictional force at the wall; and σ_x and σ_r are the stresses in the solid phase acting in the axial and radial directions, respectively. Force balance: $\Delta \sigma_x \pi R^2 = \Delta P \pi R^2 + \Delta \sigma_g \pi R^2 - \sigma_w 2 \pi R \Delta x$; $\Delta \sigma_g = (\rho_s - \rho_l)(1 - \epsilon) g \Delta x$; $\Delta P = \mu U_o \Delta x / k$; $\sigma_w = \mu_f \sigma_r = \mu_f K \sigma_x$.

Previously, the flow through compressible filter cakes and chromatographic beds has been modeled using one-dimensional models. Jostrua et al. (1967), Davies and Bellhouse (1989) and Mohammad et al. (1992) used exponential functions to directly correlate the solid stress to the permeability. These exponential correlations do not distinguish between the purely mechanical and hydrodynamic properties, that is, the change in void volume due to compression and the changes in flow pattern due to the structural changes in the chromatographic column, which are properties required to calculate the velocity field (U).

Shirato et al. (1968), Verhoff and Furjanic (1983), and Davies and Bellhouse (1989) used the Janssen approach to model the side-wall friction in compression–permeability cells and chromatographic columns, respectively. The Janssen approach (e.g., McCabe and Smith, 1983) was originally developed in order to calculate the solid stress in hoppers in the static case. The Janssen theory is based on the integration of the forces acting on an axial segment of the column. The net force acting on an axial segment of the column is the sum of the viscous forces caused by the flow, the gravitational forces, and the frictional forces ($C_w = 0$) at the wall, according to Figure 1. The viscous forces during chromatographic flow were calculated from Darcy's law (Eq. 1) (Verhoff and Furjanic, 1983; Davies and Bellhouse, 1989).

Rigorous two-dimensional models

Two distinct groups of models can be used to model the behavior of a particulate mass: those with constitutive laws based on plasticity, and those without. Our main interest is in modeling the chromatographic bed after it has been mechanically conditioned, that is, when the plasticity is negligible. In this case, the deformation can be described by a model based on pure elastic analysis. The elastic behavior of a granular material is generally isotropic, and the Poisson ratio (ν) is

practically constant at a given void ratio, while Young's modulus (E) and the shear modulus (G) are functions of the state of the compression (Lade and Nelson, 1987).

A general three-dimensional model for small deformations in a consolidating isotropic porous medium, assuming pure elastic deformations, was first derived by Biot (1941). The theory of Biot is based on the validity of Darcy's law (Eq. 1) and Hooke's law. The model is directly applicable to linear systems, but may also be applied to model incremental variations in nonlinear systems; the latter case has been discussed by e.g. Lewis and Schrefler (1987).

The Model

A model based upon the theory of Biot (1941) was previously developed by Östergren and Trägårdh (1997) and is summarized in this section. The effective stress principle (Terzaghi, 1923) is applied, which states that the deformation is caused by the intergranular forces and that the surrounding fluid pressure will not contribute to the deformation. The change in volume of the particles is assumed to be negligible under chromatographic flow conditions. The solid phase is considered to be locally isotropic, and the deformation is assumed to be described by Hooke's law. The elastic properties are described as functions of the void fraction. The gel is assumed to be saturated with water and the water-flow through the interstitial space is described by Darcy's law (Eq. 1). Steady-state and axial symmetry are assumed. Expressed in cylindrical polar coordinates (Verruijt, 1969), the equation for calculating the displacement in the axial direction (u_x) (Östergren and Trägårdh, 1997) becomes

$$\frac{1}{r}\frac{\partial}{\partial r}\left[rG\frac{\partial u_x}{\partial r}\right]+\frac{\partial}{\partial x}\left[(2G+\lambda)\frac{\partial u_x}{\partial x}\right]+\frac{1}{r}\frac{\partial}{\partial r}\left[rG\frac{\partial u_r}{\partial x}\right]+\frac{\partial}{\partial x}\lambda\left[\frac{\partial u_r}{\partial r}+\frac{u_r}{r}\right]=\frac{\partial P}{\partial x}, \quad (4)$$

and the equation to be solved in order to calculate the displacement in the radial direction (u_r) becomes

$$\frac{1}{r}\frac{\partial}{\partial r}\left[r(2G+\lambda)\frac{\partial u_r}{\partial r}\right]+\frac{\partial}{\partial x}\left[G\frac{\partial u_r}{\partial x}\right]-u_r\left[\frac{2G+\lambda}{r^2}-\frac{1}{r}\frac{\partial \lambda}{\partial r}\right]+\frac{\partial}{\partial r}\left[\lambda\frac{\partial u_x}{\partial x}\right]+\frac{\partial}{\partial x}\left[G\frac{\partial u_x}{\partial r}\right]=\frac{\partial P}{\partial x}, \quad (5)$$

where λ is Lame's coefficient:

$$\lambda=\frac{\nu E}{(1-2\nu)(1+\nu)}, \quad (6)$$

and G is the shear modulus, which is related to Young's modulus (E) and the Poisson (ν) ratio according to

$$G=\frac{E}{2(1+\nu)}. \quad (7)$$

The fluid stress was calculated in accordance with the usual convention (e.g., Verruijt, 1969; Lewis and Schrefler, 1987)

Table 1. Boundary Conditions for the Solid-Phase Equations

Inlet	$x = H$ $u_r(r, H) = 0$ $\partial u_x(r, H)/\partial x = 0$
Outlet	$x = 0$ $u_x(r, 0) = 0$ $\partial u_r(r, 0)/\partial x = 0$
Center	$r = 0$ $u_r(0, x) = 0$ $\partial u_r(0, x)/\partial r = 0, \quad \partial u_x(0, x)/\partial r = 0$
Wall	$r = R$ $u_r(R, x) = 0$ $\sigma_w(x) = \mu_f \sigma_r(R, x)$

by combining the continuity equation for one-phase flow under the assumption of steady state:

$$\nabla\cdot(\rho U_0) = 0, \quad (8)$$

with Darcy's law (Eq. 1), assuming local isotropy, which leads to the following:

$$\nabla\cdot\left[\frac{k\rho}{\mu}\nabla P\right]=0. \quad (9)$$

Equations 4, 5 and 9 form a system of coupled equations, which were solved numerically (Östergren and Trägårdh, 1997) using a control-volume method. The boundary conditions imposed on the solid phase are summarized in Table 1 and those imposed on the fluid phase in Table 2. For the solid phase it was assumed that all stresses and strains were zero at the top, leading to zero displacement in the radial direction and zero strain ($\partial u_x/\partial x$) in the axial direction. At the outlet, the displacement in the axial direction was defined to be zero. The sample radius is constant, thus the displacement, u_r, was set to zero both at the center and at the column wall. The assumption of axial symmetry and wall friction gives the additional boundary conditions in Table 1. In the flow calculations (Table 2) the hydrodynamic pressure drop was used as an initial value.

The local permeability coefficient was calculated from the Kozeny–Carman model:

$$k=\frac{d_p^2}{C_{kc}}\frac{\epsilon^3}{(1-\epsilon)^2} \qquad C_{kc}=180, \quad (10)$$

Table 2. Boundary Conditions for the Fluid-Phase Equations

Inlet	$x = H$ $P(r, H) = \Delta P_{\text{column}}$
Outlet	$x = 0$ $P(r, 0) = 0$
Center	$r = 0$ $\partial P(0, x)/\partial r = 0$
Wall	$r = R$ $\partial P(R, x)/\partial r = 0$

which relates the void fraction and the particle diameter to the permeability (Bear, 1972). The model was found to describe the permeability well for chromatographic flow conditions using spherical glass beads (Östergren and Trägårdh, 1990).

The stress originating from gravitational forces (Δg, according to Figure 1) was small compared with the other terms and could be neglected in the simulations.

Materials and Methods

Sephadex G-75 (Pharmacia Biotech, Sweden) was used as the experimental medium. The water content of the particles does not depend on the ionic strength of the liquid phase (Pharmacia, 1990) and is not sensitive to mechanical load. Flodin (1963) used centrifugation of the gel (1,000–2,000 rpm, $r = 0.15$ m) to remove the intergranular pore water before calculating the water absorbed by the gel particles. A rough approximation of the pressure exerted on the bottom of the centrifugal tube, assuming the height of the packed gel-particles to be 1 cm and a centrifugation speed of 1,000 rpm, gives a stress about one magnitude higher than the highest stress exerted on the gel in the present study. At compression, the particles will not deform permanently (e.g., Ueyama and Furusaki, 1985).

The density of the gel particles was approximately 1,040 kg/m^3 (Flodin, 1963). The mean particle diameter was determined by photomicrography. The number mean wet particle diameter was 144 μm and the area mean diameter was 178 μm. The volume of the solid phase/kg dry gel was 9.95 L. This value was obtained by subtracting the void volume from the total bed volume, using a column packed with a known amount of gel (dry weight). The void volume was determined by measuring the ratio of superficial to interstitial velocity using a marker that was totally excluded from the gel (dextran sulphate, MW = 500,000). All experiments were performed using deaerated and deionized water containing 3×10^{-4} M NaCl.

Mechanical characterization

The gel was mechanically characterized using a cubic plane strain tester, originally developed by Arthur et al. (1985) and later refined by Ogunbekun (1988). This instrument is used in order to investigate the strength/deformation characteristics of powders at extremely low stress levels (< 15 kPa) and large displacements. The cubic plane strain tester used to test the gel had been further improved by Maltby (1993) (see Figure 2a).

The shape of the sample in the cubic plane strain tester is rectangular. Deformation is allowed to occur in two directions, while the third dimension is kept constant. The inner walls of the cubic-plane strain tester are covered with membranes. The membranes are constructed so that they will not move relative to the sample, to ensure that there are no interfering frictional forces. The stress can be varied freely in two directions (Figure 2b), while the stress in the third direction is a function of the stress applied. A cylindrical filter was introduced into the original cell in order to perform measurements on a water-saturated sample. The filter was connected to a container filled with water. The pore pressure, which was kept constant and close to atmospheric pressure throughout the experiments, was regulated by elevating and lowering the water container. An initial gel concentration of approximately 66 g dry gel/L was used. The gel was carefully transferred to the cubic plane strain tester in order to avoid entrapped air. Equal stresses (σ_x, σ_y) were then applied to the sample. The deformations in the x- and y-directions and the stress in the z-direction were recorded. The deformation as a function of time in a typical experiment is shown in Figure 3a, and the stress recordings are shown in Figure 3b. The peak in the σ_z-recordings at the beginning of each stress level

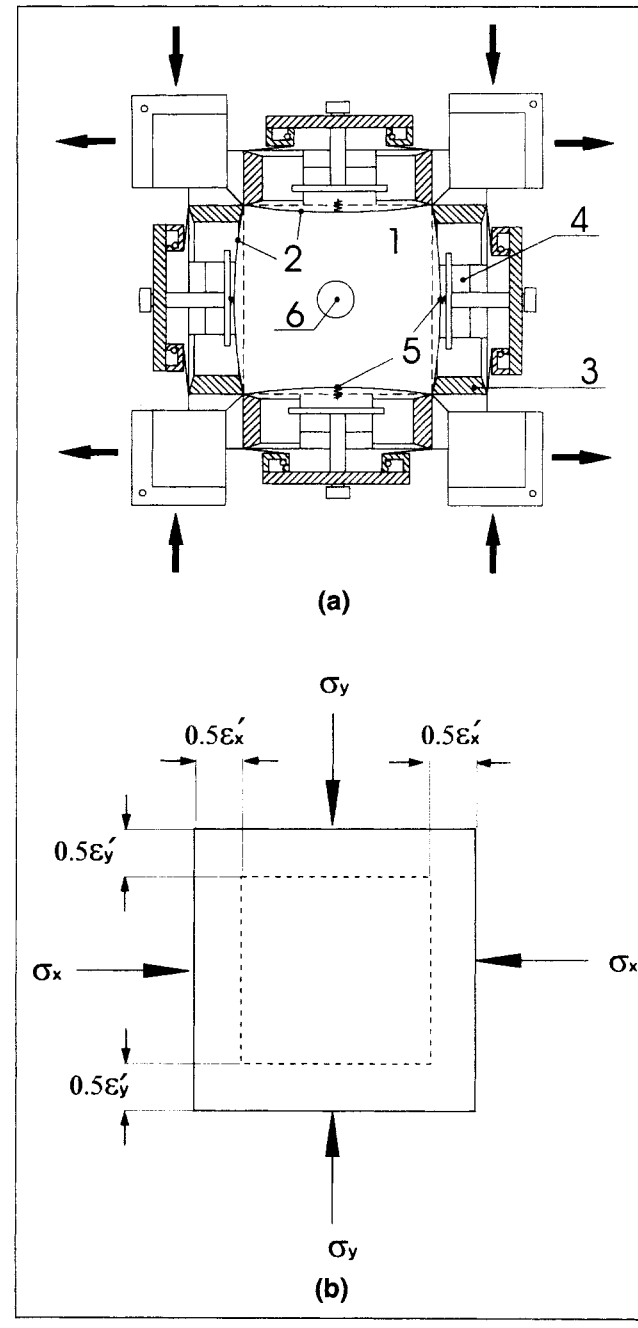

Figure 2. Cubic plane strain tester.

(a) 1. Sample; 2. flexible membranes; 3. expandable frame; 4. load stress (air pressure); 5. small spring, acting as an on/off switch; 6. filter; (b) stresses (σ_x, σ_y) and corresponding strains (ϵ_x', ϵ_y') acting in the biaxial direction.

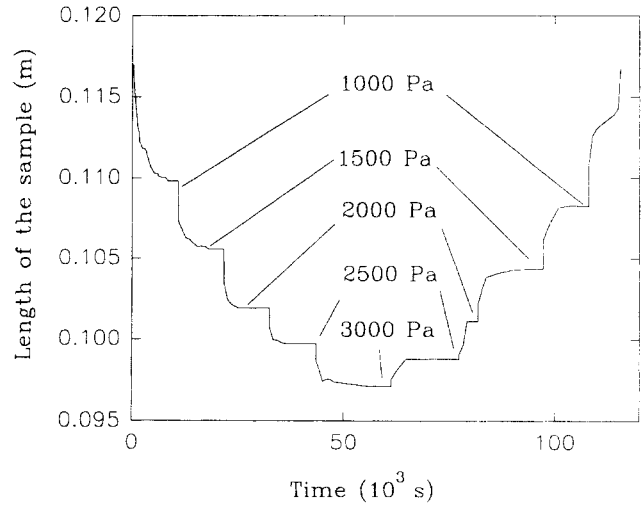

(a)

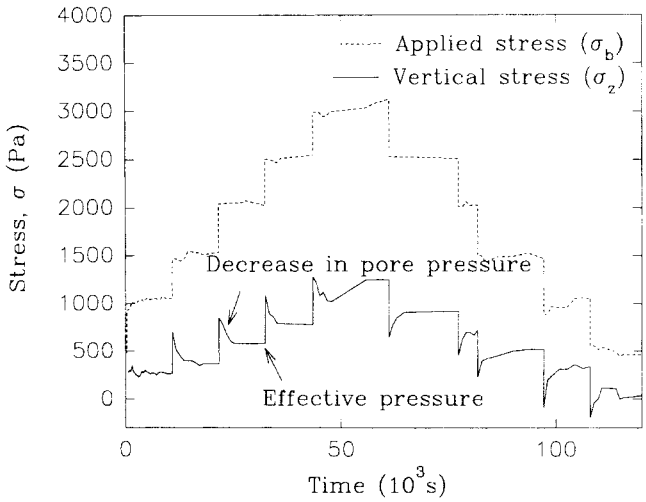

(b)

Figure 3. Experimental recordings using the cubic plane strain tester: (a) displacement recordings; (b) stress recordings.

is due to the increase in pore pressure as the sample is deformed. At steady state, when all excess water has left the sample, the pressure on the membranes corresponds to the solid stress.

The tangential Young modulus (E) and the corresponding Poisson ratio (ν) were calculated from the experiments by applying Hooke's law for successive incremental stress intervals according to

$$\frac{\Delta l_x}{l_x} = \frac{1}{E}[\Delta\sigma_x - \nu(\Delta\sigma_y + \Delta\sigma_z)] \tag{11}$$

$$\frac{\Delta l_y}{l_y} = \frac{1}{E}[\Delta\sigma_y - \nu(\Delta\sigma_z + \Delta\sigma_x)] \tag{12}$$

$$\frac{\Delta l_z}{l_z} = \frac{1}{E}[\Delta\sigma_z - \nu(\Delta\sigma_y + \Delta\sigma_x)], \tag{13}$$

where Δl_x, Δl_y, Δl_z are the incremental deformations for a given stress interval. The experimental conditions in the cubic plane strain tester imply

$$\sigma_x = \sigma_y = \sigma_b \tag{14}$$

$$\frac{\Delta l_x}{l_x} = \frac{\Delta l_y}{l_y} \tag{15}$$

$$\Delta l_z = 0, \tag{16}$$

leading to

$$\nu = \frac{\Delta\sigma_z}{2\Delta\sigma_b} \tag{17}$$

and

$$E = \frac{l_x \Delta\sigma_b}{\Delta l_x}(1 - \nu - 2\nu^2). \tag{18}$$

The void fraction was calculated from the amount of dry gel and water content at the end of the experiments. Samples were taken from different positions in the measuring cell. Care was taken to obtain the same particle concentration in the sample as in the cell. The samples were dried to a constant weight at 105°C. The volume fraction of each phase was then calculated.

Wall shear stress

The wall shear stress was measured using a Jenike shear cell (Jenike, 1964) totally submerged in water. The lid of the shear cell was modified so it was kept in contact with the gel as the gel was successively compacted. The normal stress was varied between 1 and 6 kPa. The sample was sheared at a speed of 0.0448×10^{-3} m/s. The samples were left to rest for a few minutes between each measurement. The wall friction coefficient was calculated from

$$\mu_f = \frac{T}{N}, \tag{19}$$

where N is the normal force and T the shear force.

Column experiments

The column experiments were performed in a commercial chromatographic column (oxirane-glass) with a diameter of 0.113 m (BP113, Pharmacia Biotech, Sweden). The amount of solid phase was the same in all experiments, corresponding to a height of 0.13 m at zero void fraction. The experimental setup is shown in Figure 4. In order to measure the pressure profile along the column, six holes ($d = 1$ mm) were drilled. A net of fine-mesh polyester was placed across the hole to prevent the gel from leaking out. The holes were connected to a pressure board by tubing and then to a pressure transducer, as shown in Figure 4. The adapter was mounted just above the gel surface so there would be no additional forces

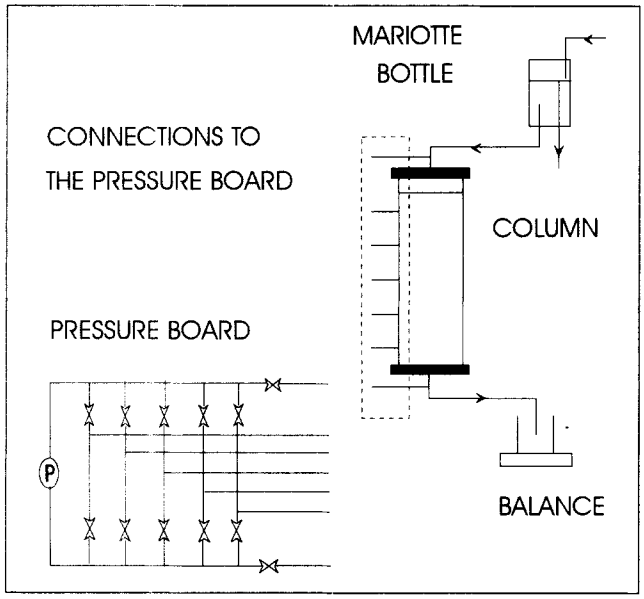

Figure 4. The experimental setup used in the column experiments.

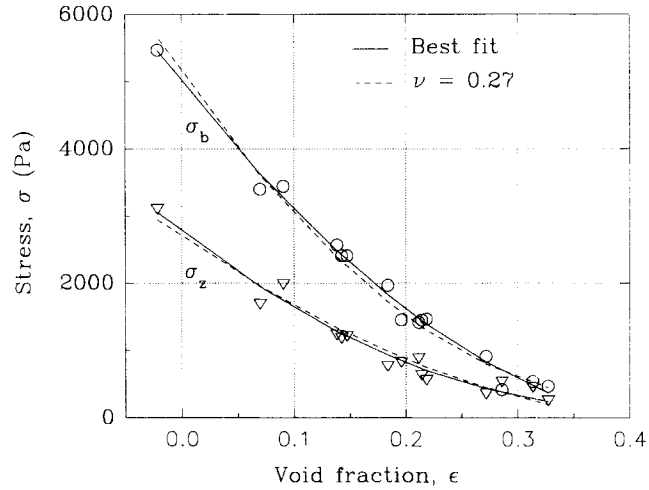

Figure 5. Horizontal (σ_b) and vertical stress (σ_z) as a function of the void fraction using the cubic plane strain tester.

on the gel. A Mariotte bottle was used to ensure a pulse-free flow. The pressure head was determined by the elevation of the Mariotte bottle. The experiments were performed at room temperature. The temperature was measured using a thermocouple at the outlet of the column. The data were corrected for temperature variations between the experiments. The reference temperature used was 20.0°C. The mass flow rate was continuously monitored using a balance connected to a computer. The column was filled with a thick slurry made up of three volumes Sephadex gel and one volume supernatant. The gel was then allowed to sediment overnight. The pressure was increased stepwise and the flow rate was recorded; all measurements were taken at steady state. For each pressure head, the column height, the hydrodynamic pressure drop, the flow rate, and the outlet temperature were measured. Corrections were made for the extra column pressure drop caused by the endpieces of the column.

Results and Discussion

Mechanical properties

No differences were observed between successive compression–recovery cycles using the cubic plane strain tester, from which it can be concluded that a stable packing structure was established before the first measurement was made. A small hysteresis in the compression–recovery cycles having a maximum value of $[(\sigma_b)_{comp.}-(\sigma_b)_{relax}]/(\sigma_b)_{comp.}=0.2$ was found. Hysteresis is to be expected because some pressure gradient is required to make liquid flow in and out of the voids according to the volume changes. During compression this gives an additional stress, whereas during expansion it results in a reduction. The hysteresis will decrease with decreasing rate of change in stress, but in these experiments, which were carried out extremely slowly (see Figure 3), it seems to approach an asymptotic residue, which may be caused by particle interlocking.

The results, which are based upon three experimental series, are shown in Figure 5. The compression data were fitted to a second-order equation and the Poisson ratio and the tangential Young's modulus were calculated according to Eqs. 17 and 18, respectively. The results are presented in Table 3. The precision of the experimental results (Figure 5) was not sufficient to correlate the Poisson ratio to the void fraction, so that the Poisson ratio was approximated to be a constant value. The approximation was validated by recalculating σ_b and σ_z from the fitted values of σ_z and σ_b, respectively, using Eq. 17 (Figure 5).

Young's modulus was correlated to the void fraction, which can be done for packed beds having the same packing structure. It is assumed that the successive compaction and relaxation of the packing during the column experiments will cause the particles to adapt to a close random packing, which for a packed bed of rigid particles is characterized by a void fraction between 0.32 and 0.375, depending on the size distribution (Greenkorn, 1983). This agrees well with our experimentally determined void fraction for the completely relaxed bed, which was 0.358. In the cubic plane strain tester we believe that the extremely slow compaction allows the particles to slide into a similar packing pattern.

The apparently negative void fraction at high loads shows that the bed volume has changed more than the interstitial pore-space allows for, which is an indication of a small change in the particle volume as the bed is compressed.

Wall shear stress

The results of the wall shear stress measurements are shown in Figure 6. The data are correlated by a straight line

Table 3. Young's Modulus (E), the Poisson Ratio (ν), and the Wall Friction Coefficient (μ_f) of the Gel

E (Pa)	ν	μ_f
$E=5.63\times10^4\cdot\epsilon^2-8.39\times10^4\cdot\epsilon+2.77\times10^4$	0.27	0.16

ϵ = void fraction.

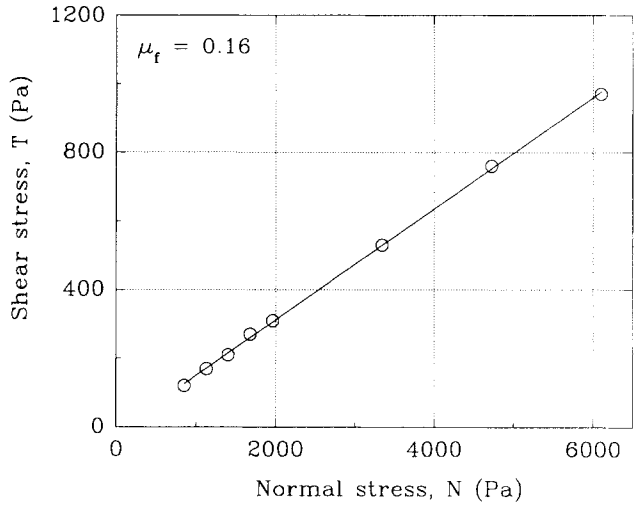

Figure 6. Wall shear-stress measurements using the modified Jenike shear cell.

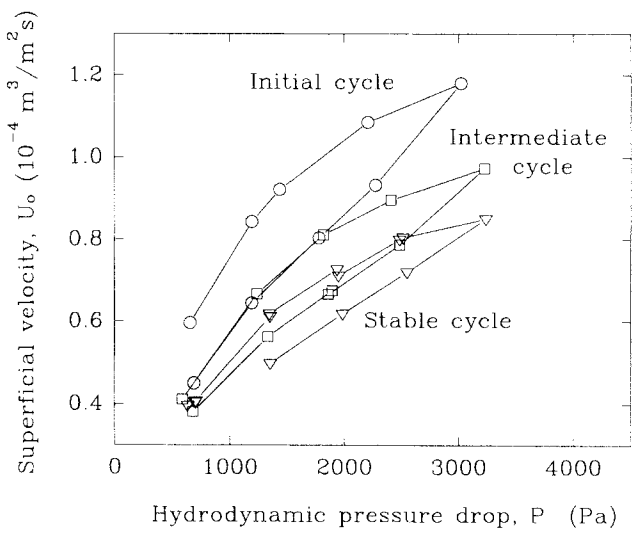

Figure 8. Flow measurements for an initial, an intermediate, and a stable compression-recovery cycle.

passing close to zero, which indicates that the adhesion of the gel to the wall was negligible, and that the variation in the wall friction coefficient with load was negligible. The wall friction coefficient was found to be 0.16 (Table 3).

Column experiments

The stability of the gel was investigated by performing cyclic experiments. The time required to attain steady-state and the reproducibility of the experiments were determined. The pressure drop along the chromatographic column was measured as well.

Data from a typical experiment are shown in Figures 7 and 8. The time required to reach steady-state was 10–15 min. In most cases, the packed bed was mechanically stable after 4–5 cycles. The achievement of a mechanically conditioned packing confirms that the initial plastic deformation is due to irreversible rearrangement of the particles. The hysteresis in the column is partly due to the different Young's modulus and Poisson ratios of the gel at compression and relaxation, which was seen in the biaxial experiments. Computer simulations (not shown), using the mechanical properties extracted from the relaxation data using the cubic plane strain tester gave a hysteresis of the same size as in Figure 8. However, the shape of the curve describing the relaxation was more convex than that obtained experimentally. This indicates that the different stress situation in the column due to the shear stresses induced by the wall friction may be of importance when determining the Young's modulus and the Poisson ratio at relaxation. The stability of the mechanically conditioned packing was investigated by increasing the pressure head, typically to one and a half times the previously applied maximum pressure head. The flow-pressure curve thus obtained coincided with the previous curve, which confirms that the chromatographic column deforms purely elastically over a broad pressure range.

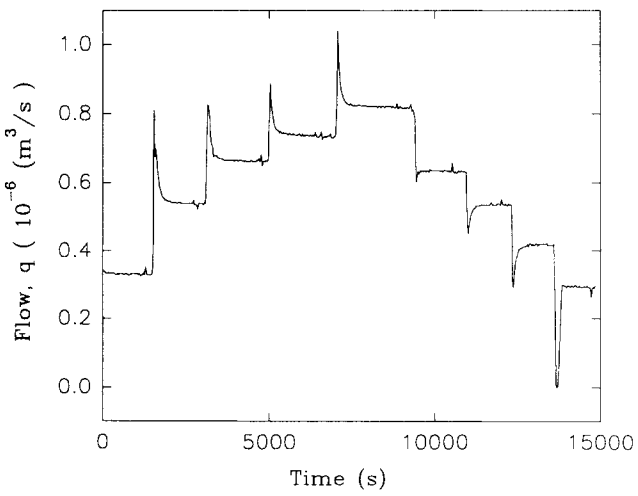

Figure 7. Typical experimental recordings from a compression-recovery cycle.

The pressure range was 0.6×10^3–3.2×10^3 Pa.

Experiments were performed in triplicate using the same gel concentration. Highly reproducible (stable) packing behavior was observed, although the initial structures were different (Figure 9).

Computer simulations

Computer simulations were performed for the open-column situation in order to confirm the model (Table 3) describing the compaction of the gel and to qualitatively investigate the structural changes of the gel at different degrees of compaction. The initial void fraction was 0.358, according to the experimental measurements. The column dimensions and the parameters of Eqs. 9 and 10 describing the flow are summarized in Table 4. The void fraction was calculated from the change in volume strain (Biot, 1941), assuming a constant particle volume.

Computed and experimentally determined pressure profiles, column heights, and flow rates are shown in Figure 10. The calculated pressure profiles and the calculated column

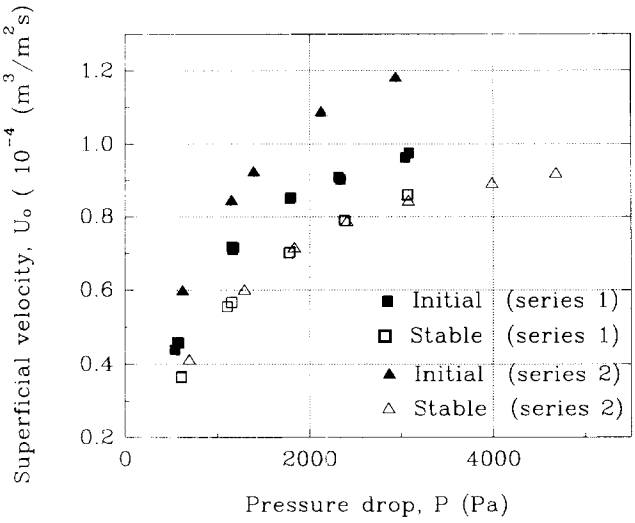

Figure 9. Reproducibility of the compression stage of two successive experimental series.

heights are in good agreement with the experimentally determined values (Figures 10a and 10b). Approximately half the pressure drop is found in the last 20% of the column, at the highest pressure head, which shows that the permeability decreases rapidly at the bottom of the column. This is in accordance with experimental and theoretical results in the literature (e.g., Jostrua et al., 1967; Verhoff and Furjanic, 1983). The predicted flow rates were approximately 30% higher than those measured (Figure 10c). The difference in predicted and measured flow rates is most likely dependent on the permeability model. The Kozeny–Carman model (Eq. 10) is based upon the assumption that the solid phase surface area is constant, which means the particles remain spherical. Previously it has been shown that a compressed sample of Sephadex gel has a reduced solid-phase surface area (Ueyama and Furasaki, 1985). It has also been shown that a consolidated granular medium has an increased tortuosity (Barci et al., 1987). Using the original Kozeny–Carman model (Eq. 10) thus leads to an underestimation of the permeability of a medium with a decreased solid-phase surface area and an overestimation of the permeability of a medium with an increased tortuosity (Bear, 1972). The presented results, if interpreted according to the Kozeny–Carman model, led to the conclusion that the change in tortuosity dominates over the change in surface area. Excellent agreement between measured and simulated flow rates was obtained by using a constant of valve 240 in Eq. 10 (Figure 10c).

The model using a constant of 240 in Eq. 10 was also tested by varying Young's modulus (by varying the σ_b-correlation in Figure 5, within the 95% confidence limits), the Poisson's ra-

Table 4. Additional Parameters Used in the Computer Simulations

Col. Radius (m)	Init. Col. Height (m)	Init. Void Fraction	Particle Dia. (m)	Visc. (Pa·s)	Fluid Density (kg/m^3)
0.0565	0.199	0.358	178×10^{-6}	0.001	1000

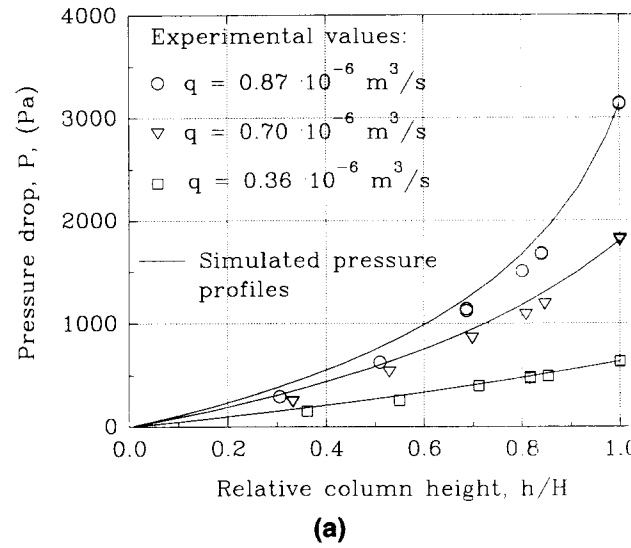

(a)

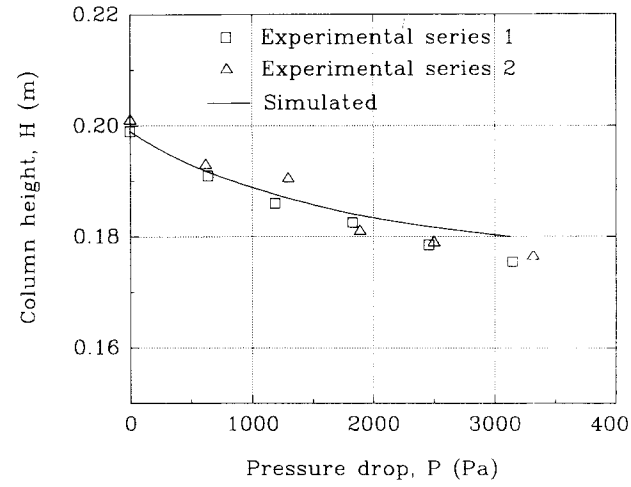

(b)

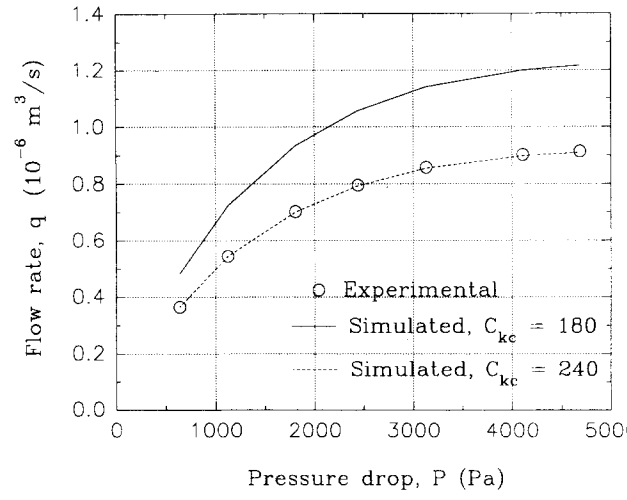

(c)

Figure 10. Computed and experimentally determined (a) pressure profiles; (b) column heights; (c) and flow rates.

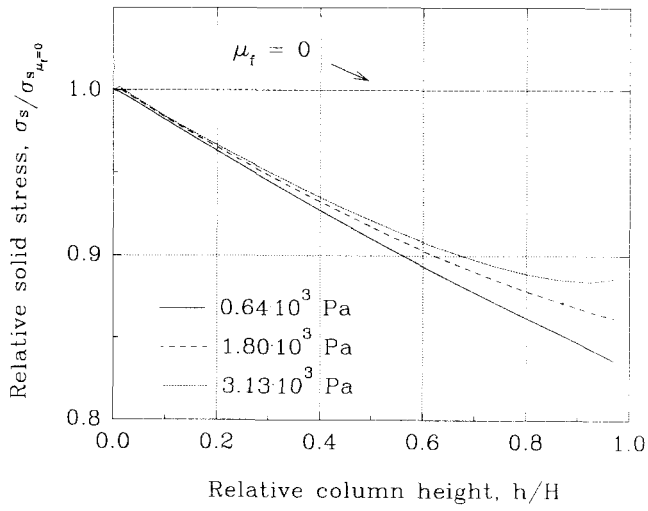

Figure 11. Computed relative solid stress at different degrees of compaction.

tio (0.25 and 0.3), and finally by varying the wall friction coefficients (0.14 and 0.18). The values reflect the estimated accuracy of the experimentally determined coefficients. Both the variation in Young's modulus and the Poisson ratio caused a systematic pressure-dependent error in the predicted flow rates. The error was less than 10%. The variation in the wall friction coefficient caused very small changes in the predicted flow rates and pressure profiles.

The model presented here offers the opportunity of qualitatively investigating the structural changes in the column at different degrees of compaction. Figure 11 shows the computed solid stress in the axial direction relative to the solid stress at zero wall friction. Ideally, at zero wall friction, the whole pressure drop is taken up by the solid phase. The reduction of the solid stress at the bottom of the column is in the 10–15% range and will be larger for narrow columns and smaller for wider columns. The largest reduction of solid stress was found at the lowest degree of compaction and vice

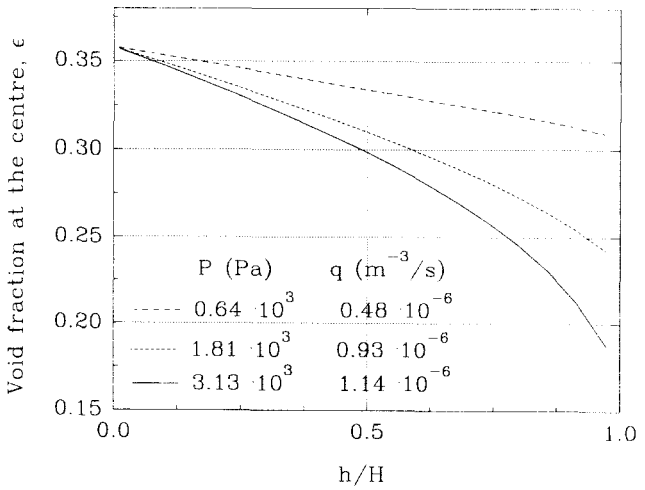

Figure 12. Computed void variation at the center of the column at three different degrees of compaction.

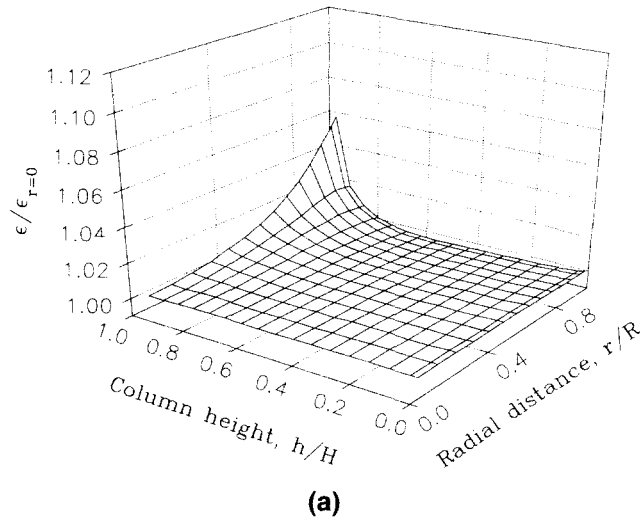

(a)

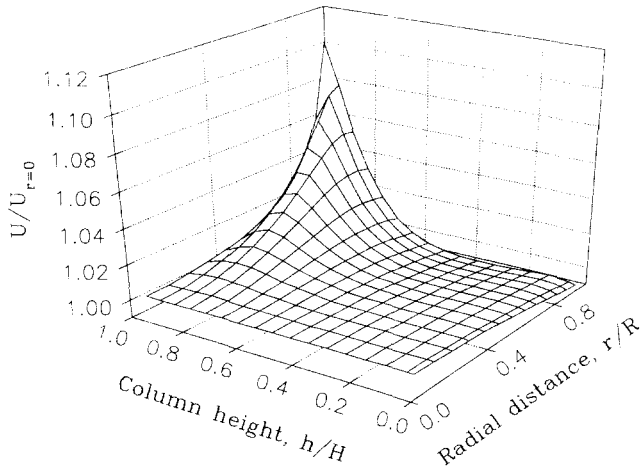

(b)

Figure 13. Computed (a) void variations relative to the central void fraction, and (b) corresponding variations in linear velocity.

$P = 3.13 \times 10^3$ Pa; $q = 1.14 \times 10^{-6}$ m^3/s.

versa. This is due to the successively increased degree of compaction at the bottom of the column as the pressure head is increased. At a high pressure head/high flow rate most pressure is lost in a small region close to the outlet of the column, and the surface of the wall available to take up a given fraction of the stress is smaller than the surface available to take up the same fraction of stress in a more homogeneously packed column.

Simulated variations of the void fraction in the axial direction are shown in Figure 12. At the lowest degree of compaction, the packed bed is almost homogeneous, while at the highest degree of compaction the void ratio is predicted to vary between 0.36 at the inlet and 0.2 at the outlet. The radial void variations and the corresponding axial velocity variations are shown in Figures 13a and 13b, respectively. The simulations show that a radial void profile is developed in approximately the last 20% of the column as the pressure head/flow rate is increased. The variations in void fraction

and linear velocity were 6% and 12%, respectively, at the highest flow rate, according to Figure 13. At lower flow rates the variations were smaller.

Summary and Conclusions

Experiments performed in a chromatographic column show that the dextran-based Sephadex gel deforms purely elastically, and that it is possible to reproduce a stable packing pattern, qualities that are essential in order to successfully model the system.

A method was developed to characterize a water-saturated gel under well-controlled conditions using a cubic plane strain tester, originally developed for characterizing dry powders. A small hysteresis was found in the compression–recovery cycles. The state of compression was carefully analyzed. Young's modulus was determined as well as Poisson's ratio. The Young's modulus was found to be strongly dependent on the void fraction. The Poisson ratio could be approximated by a constant value.

The wall friction coefficient was determined using a Jenike shear cell, which was modified so that water-saturated samples could be analyzed. The shear test showed that the wall friction did not vary with the degree of compaction and that the adhesion to the wall was negligible.

A two-dimensional mathematical model based on the mechanical characteristics of the gel was presented. The model is based on a purely elastic analysis of a locally isotropic granular medium (Biot, 1941) and on the validity of Darcy's law. The coupled equations were solved numerically using a control-volume method.

The simulated pressure profiles agreed well with the experimental data. The predicted flow rates were approximately 30% higher than the experimental values. Using a constant of value 240 in the Kozeny–Carman equation (Eq. 10), the experimental and calculated values agreed very well.

Simulations of axial and radial void variations as well as variations in the linear velocity (U) across the column show that the use of a two-dimensional model may be a helpful tool in gaining further insight into the chromatographic process using nonrigid chromatographic media.

Acknowledgments

The authors acknowledge the Swedish Board for Technical and Industrial Development for financial support, and Pharmacia Biotech AB for supplying them with chromatographic medium and chromatographic columns. The authors are also grateful to Dr. Lars Petter Maltby who made the necessary modifications to the cubic plane strain tester and made the initial measurements, and to Mrs. Wenche Bergland Fougner, POSTEC Research A/S, who carried out the wall shear-stress measurements.

Notation

C_{kc} = coefficient in Eq. 10
d_p = particle diameter
H = column height
h = distance from the column inlet
K = coefficient relating radial and axial stresses
P = pressure (Eq. 2)
R = column radius
r = radial distance
t = time
ϵ' = strain in the solid phase

Subscripts

b = biaxial stress
s = solid phase
l = liquid phase
r, x = coordinate directions in a circular cylindrical coordinate system

Literature Cited

Arthur, J. R. F., T. Dunstam, and G. G. Enstad, "Determination of the Flow Function by Means of a Cubic Plane Strain Tester," *Int. J. Bulk Storage Silos*, **1**(2), 7 (1985).

Barci, J.-C., N. Rakotomalala, and D. Salin, "Experimental Evidence of Disorder Effects in Hydrodynamic Dispersion," *Phys. Rev. Lett.*, **58**, 2035 (1987).

Bear, J., *Dynamics of Fluids in Porous Media*, American Elsevier, New York (1972).

Biot, M. A., "General Theory of Three-Dimensional Consolidation," *J. Appl. Phys.*, **12**, 155 (1941).

Bird, B. R., W. E. Stewart, and E. N. Lightfoot, *Transport Phenomena*, Wiley, New York (1960).

Boschetti, E., "Review: Advanced Sorbents for Preparative Protein Separation Purposes," *J. Chromatogr.*, **658**, 207 (1994).

Charlaix, E., J. P. Hulin, and T. J. Plona, "Experimental Study of Tracer Dispersion in Sintered Glass Porous Materials of Variable Compaction," *Phys. Fluids*, **30**, 1690 (1987).

Davies, P. A., and B. J. Bellhouse, "Permeability of Bed of Agarose-Based Particles," *Chem. Eng. Sci.*, **44**, 452 (1989).

Flodin, P., *Dextran Gels and Their Applications in Gel Filtration*, Meijels Bokindustri, Halmstad, Sweden (1963).

Greenkorn, R. A., *Flow Phenomena in Porous Media Fundamentals and Applications in Petroleum, Water and Food Production*, Dekker, New York (1983).

Jenike, A. W., "Storage and Flow of Solids," *Bulletin No. 123*, Utah Engineering Experiment Station, Univ. of Utah (1964).

Jönsson, K. A.-S., and B. T. L. Jönsson, "Fluid Flow in Compressible Porous Media: I. Steady-State Conditions," *AIChE J.*, **38**, 1340 (1992).

Jostrua, M. K., A. Emnéus, and P. Tibbling, "Large-Scale Gel Filtration," *Protides of the Biological Fluids*, Vol. 15, H. Peeters, ed., Elsevier, Amsterdam, p. 575 (1967).

Lade, P. V., and R. B. Nelson, "Modelling the Elastic Behaviour of Granular Materials," *Int. J. Numer. Anal. Methods. Geomech.*, **11**, 521 (1987).

Lewis, R. W., and B. A. Schrefler, *The Finite Element Method in the Deformation and Consolidation of Porous Media*, Wiley, Great Britain (1987).

Maltby, L. P., "Investigation of the Behaviour of Powders under and after Consolidation," Dr. Ing. Thesis, Telemark College, Porsgrunn, Norway (1993).

McCabe, W. L., and J. C. Smith, *Unit Operations of Chemical Engineering*, McGraw-Hill, Tokyo, p. 809 (1983).

Mohammad, A. W., D. G. Stevenson, and P. C. Wankat, "Pressure Drop Correlations and Scale-Up of Size Exclusion Chromatography with Compressible Packings," *Ind. Eng. Chem. Res.*, **31**, 549 (1992).

Ogunbekun, O. O. O., "The Influence of Boundary Constraints on the Shearing Characteristics of Particulate Solids at Extremely Low Stress Levels," PhD Thesis, Univ. College, London (1988).

Östergren, K., and C. Trägårdh, "A Study of Permeability and Hydrodynamic Dispersion under Conditions of Chromatographic Flow," *Separations for Biotechnology*, D. L. Pyle, ed., Elsevier, Great Britain, p. 632 (1990).

Östergren, K. C. E., and C. Trägårdh, "Numerical Study of Two-Dimensional Compaction Flow and Dispersion in a Chromatographic Column," *Numer. Heat Transfer, Part A*, **32**, 247 (1997).

Pharmacia LKB Biotechnology, *Gel Filtration Theory and Practice*, Lund, Sweden (1990).

Shirato, M., T. Aragaki, R. Mori, and K. Sawamoto, "Predictions of Constant Pressure and Constant Rate Filtrations Based upon an Approximate Correction for Side Wall Friction in Compression Permeability Cell Data," *J. Chem. Eng. Jpn*, **1**, 86 (1968).

Sofer, G. K., and L. E. Nyström, *Process Chromotography, A Practical Guide*, Academic Press, London (1989).

Terzaghi, K., "Die Berechnung der Durchlässigkeitziffer des Tones aus dem Verlauf der Hydrodynamichen Spannungserscheinungen," *Akad. Wiss. Wien, Sitzungsber. math.-naturwiss. Kl.*, Part IIa, **132**(3/4), 125 (1923).

Tiller, F. M., and W.-M. Lu, "The Role of Porosity in Filtration VIII Cake Nonuniformity in Compression-Permeability Cells," *AIChE J.*, **18**, 569 (1972).

Ueyama, K., and S. Furasaki, "A Theoretical Study on the Effect of Compaction on the Effectiveness Factor on Gel Particles Containing Immobilized Enzymes," *Chem. Eng. Commun.*, **36**, 299 (1985).

Verhoff, F. H., and J. J. Furjanic, "Compressible Packed Bed Fluid Dynamics with Application to a Glucose Isomerase Reactor," *Ind. Eng. Chem. Process Des. Dev.*, **22**, 192 (1983).

Verruijt, A., "Elastic Storage of Aquifers," *Flow Through Porous Media*, A. J. M. DeWiest, ed., Academic Press, New York, p. 331 (1969).

Yun, T., and G. Guiochon, "Modeling of Radial Heterogeneity in Chromatographic Columns, Columns with Cylindrical Symmetry and Ideal Model," *J. Chromatogr.*, **672**, 1 (1994).

Manuscript received Nov. 26, 1996, and revision received Sept. 23, 1997.